E7386, a Selective Inhibitor of the Interaction between β-Catenin and CBP, Exerts Antitumor Activity in Tumor Models with Activated Canonical Wnt Signaling

Kazuhiko Yamada[1], Yusaku Hori[1], Satoshi Inoue[1], Yuji Yamamoto[1], Kentaro Iso[1], Hiroshi Kamiyama[1], Atsumi Yamaguchi[1], Takayuki Kimura[1], Mai Uesugi[1], Junichi Ito[1], Masahiro Matsuki[1], Kazutaka Nakamoto[1], Hitoshi Harada[1], Naoki Yoneda[1], Atsushi Takemura[1], Ikuo Kushida[1], Naomi Wakayama[1], Kenji Kubara[1], Yu Kato[1], Taro Semba[1], Akira Yokoi[1], Masayuki Matsukura[1], Takenao Odagami[2], Masao Iwata[1], Akihiko Tsuruoka[1], Toshimitsu Uenaka[1], Junji Matsui[3], Tomohiro Matsushima[1], Kenichi Nomoto[3], Hiroyuki Kouji[2], Takashi Owa[3], Yasuhiro Funahashi[1], and Yoichi Ozawa[1]

ABSTRACT

The Wnt/β-catenin signaling pathway plays crucial roles in embryonic development and the development of multiple types of cancer, and its aberrant activation provides cancer cells with escape mechanisms from immune checkpoint inhibitors. E7386, an orally active selective inhibitor of the interaction between β-catenin and CREB binding protein, which is part of the Wnt/β-catenin signaling pathway, disrupts the Wnt/β-catenin signaling pathway in HEK293 and adenomatous polyposis coli (*APC*)-mutated human gastric cancer ECC10 cells. It also inhibited tumor growth in an ECC10 xenograft model and suppressed polyp formation in the intestinal tract of $Apc^{Min/+}$ mice, in which mutation of *Apc* activates the Wnt/β-catenin signaling pathway. E7386 demonstrated antitumor activity against mouse mammary tumors developed in mouse mammary tumor virus (MMTV)-Wnt1 transgenic mice. Gene expression profiling using RNA sequencing data of MMTV-Wnt1 tumor tissue from mice treated with E7386 showed that E7386 downregulated genes in the hypoxia signaling pathway and immune responses related to the CCL2, and IHC analysis showed that E7386 induced infiltration of $CD8^+$ cells into tumor tissues. Furthermore, E7386 showed synergistic antitumor activity against MMTV-Wnt1 tumor in combination with anti-PD-1 antibody. In conclusion, E7386 demonstrates clear antitumor activity via modulation of the Wnt/β-catenin signaling pathway and alteration of the tumor and immune microenvironments, and its antitumor activity can be enhanced in combination with anti-PD-1 antibody.

Significance: These findings demonstrate that the novel anticancer agent, E7386, modulates Wnt/β-catenin signaling, altering the tumor immune microenvironment and exhibiting synergistic antitumor activity in combination with anti-PD-1 antibody.

Introduction

The Wnt/β-catenin signaling pathway (or canonical Wnt signaling pathway) is involved in the control of cellular processes, such as proliferation, differentiation, and motility. Consequently, this pathway is important not only for embryonic development, but also for the development, regulation, and survival of cancer cells (1, 2). Upon the binding of Wnt ligands to Frizzled family receptors on cell membrane, components of the destruction complex, including adenomatous polyposis coli (APC), glycogen synthase kinase 3β (GSK3β), and axin, are sequestered to the plasma membrane, where together they prevent degradation of β-catenin. Unphosphorylated β-catenin then translocates to the nucleus, where it forms a complex with the transcriptional factor T-cell factor/lymphoid enhancer-binding factor (TCF/LEF) and its cofactors, such as CREB binding protein (CBP) and p300, leading to target gene transcription.

Genetic alterations, such as activating mutations of the gene encoding β-catenin and loss-of-function mutation of *APC*, result in aberrant activation of the Wnt/β-catenin signaling pathway (3). These genetic alterations occur in multiple types of cancers, including hepatocellular carcinoma, colorectal cancer, anaplastic thyroid cancer, endometrial cancer, and desmoid tumors (4–9), and so it has been suggested that the activated Wnt/β-catenin signaling pathway is a potential novel therapeutic target. In addition, aberrant activation of the Wnt/β-catenin signaling pathway results in the development of abnormal tumor microenvironments related to tumor immunity, angiogenesis, and metabolism (10–13), and it has been reported that aberrant activation of the Wnt/β-catenin signaling pathway in tumor cells prevents T-cell infiltration into tumors by decreasing the expression of the chemokines necessary for lymphocyte migration (14, 15). Thus, the Wnt/β-catenin signaling pathway is an attractive therapeutic target, not only for direct activity against tumor cells, but also for modulation of the tumor microenvironment to enhance antitumor immunity.

Several Wnt/β-catenin signal inhibitors, including porcupine inhibitors (16), Wnt receptor antibody (17), and Wnt receptor decoy (18), have been developed (19, 20); however, these inhibitors have shown limited antitumor activity and severe toxicity in clinical trials (21, 22). It is difficult to directly target β-catenin itself by using a small

[1]Tsukuba Research Laboratories, Eisai Co., Ltd., Tsukuba, Ibaraki, Japan. [2]PRISM BioLab Co., Ltd., Kanagawa, Japan. [3]Oncology Business Group, Eisai Inc., Woodcliff Lake, New Jersey.

Note: Supplementary data for this article are available at Cancer Research Online (http://cancerres.aacrjournals.org/).

H. Kouji and T. Owa contributed equally as co-joint authors of this article.

Corresponding Authors: Yoichi Ozawa, Eisai Co., Ltd., Tokodai 5-1-3, Tsukuba, Ibaraki 300-2635, Japan. Phone: 812-9847-7096; Fax: 812-9847-7614; E-mail: y2-ozawa@hhc.eisai.co.jp; and Yasuhiro Funahashi, Phone: 812-9847-5615; Fax: 812-9847-4928; E-mail: y-funahashi@hhc.eisai.co.jp

Cancer Res 2021;81:1052–62

doi: 10.1158/0008-5472.CAN-20-0782

molecule-compound inhibitor (23), but some inhibitors, such as ICG-001 and PRI-724, which bind to CBP, inhibit the interaction of CBP with β-catenin, and consequently inhibit the function of β-catenin (24). In clinical trials, the efficacy of PRI-724 administered for 7 consecutive days or biweekly has been examined; however, PRI-724 has not yet been approved for use as anticancer drug. Therefore, novel agents targeting the Wnt/β-catenin signal transcriptional machinery are still needed to improve cancer therapy.

We discovered a novel orally active compound, E7386, that was developed by improving the microsomal stability, membrane permeability, and solubility of C-82, an active form of PRI-724. In this study, E7386 inhibited polyp formation in the intestine in $Apc^{Min/+}$ mice, and had antitumor activity in an APC-mutated ECC10 human gastric xenograft model. Mouse mammary tumor virus (MMTV)-Wnt1 transgenic mice develop spontaneous breast tumors with constitutive Wnt1 expression induced by the long terminal repeat region of MMTV. E7386 showed clear antitumor activity when administered alone and synergistic antitumor activity when administered in combination with anti-PD-1 antibody in the MMTV-Wnt1 tumor model. IHC and transcriptome analyses showed that E7386 increased the number of $CD8^+$ cells in tumor tissue and altered the immune cell population by decreasing the monocyte and M2 macrophage populations. Together, these findings showed that E7386 had antitumor activity in mouse and human preclinical models by modulating Wnt/β-catenin signaling via inhibition of the β-catenin/CBP interaction.

Materials and Methods

Compounds

E7386, ICG-001, and C-82 were synthesized by Eisai Co., Ltd., WuXi AppTec Co., Ltd., and PRISM BioLab Co., Ltd., respectively. For *in vitro* studies, compounds were prepared as 20 mmol/L stock solutions in DMSO and diluted in the relevant assay medium. For *in vivo* studies, E7386 was dissolved in 0.1 mol/L HCl, and administration volume was calculated from the body weight of each mouse (0.1 mL/10 g-body weight) before administration.

Cell lines

HEK293 cells were obtained from the ATCC, and ECC10 cells were obtained from RIKEN BioResource Center. Each cell line was cultured according to recommended culture methods and used for no more than 20 passages. ECC10 cells and HEK293 cells were tested negative for *Mycoplasma* contamination using MycoAlert Mycoplasma Detection Kit (LT07-318, Lonza) and authenticated by short tandem repeat analysis at Promega KK, or Eisai Co., Ltd. by using GenePrint 24 System (Promega), respectively.

Coimmunoprecipitation assay

FLAG-tagged N-terminal region of CBP (amino acids, 1–682) was transfected into HEK293 cells. The HEK293 transfectants, which were stimulated with 40 mmol/L of lithium chloride (LiCl), and ECC10 cells were treated with the indicated concentration of compounds for 6 hours. The treated HEK293 transfectants and ECC10 cells were lysed with 1 × Cell Lysis Buffer (Cell Signaling Technology) and an EpiQuik Nuclear Extraction Kit II (EpiGentek Group Inc.), respectively, and extracts were incubated with anti-Flag M2 Affinity Gel (Sigma-Aldrich), anti-CBP antibody, or anti-p300 antibody (Santa Cruz Biotechnology) immobilized on agarose overnight at 4°C. Proteins bound to the agaroses were eluted by boiling with SDS sample buffer and then analyzed by Western blotting.

Western blotting

For detection of acetylated β-catenin, HEK293 and ECC10 cells were treated with E7386 for 2 hours. HEK293 cells were also treated with 40 mmol/L of LiCl at the same time to increase acetylation of β-catenin. Treated cells were lysed, whole-cell extracts were separated on 5%–20% SDS–polyacrylamide gradient gels (FUJIFILM Wako Pure Chemical Corporation), and separated proteins were transferred to Nitrocellulose Membranes (GE Healthcare Life Science) by electroblotting. After blocking with TBS containing 5% nonfat dry milk and 0.1% Tween-20, the membranes were incubated individually with the following primary antibodies: acetyl-β-catenin Lys49 (#9030), glyceraldehyde 3-phosphate dehydrogenase antibody (#2118) (Cell Signaling Technology), β-catenin (H-102), CBP (A-22), and p300 (N-15) (Santa Cruz Biotechnology). The membranes were then washed and incubated with secondary horseradish peroxide anti-rabbit IgG antibody. Immunodetection was performed by using Immobilon Western Chemiluminescent HRP Substrate (Millipore) and an LAS-3000 Luminescent Image Analyzer (Fujifilm).

TCF/LEF reporter assay

We inserted three copies of the TCF/LEF binding site from TOP Flash Vector (Millipore) into either pNeo luciferase reporter plasmid, which contains the luciferase reporter gene with a mammalian selectable marker for neomycin resistance (constructed by Eisai), or pGL4.19 (Promega), to generate pNeo-TOP and pGL4.19 TOP, respectively. HEK293 cells stably transfected with pNeo-TOP or ECC10 cells transiently transfected with pGL4.19 TOP, and then transfected cells were treated with serial dilutions of E7386 for 6 hours. HEK293 cells were also treated with 40 mmol/L of LiCl at the same time to activate Wnt signaling pathway and reporter activity. TCF/LEF luciferase activity was measured with the Bright-Glo Luciferase Assay System (Promega). TCF/LEF reporter activity was determined as the ratio of luciferase activity with E7386 treatment compared with that without treatment. To determine the inhibitory activity of E7386, we also calculated the ratio of luciferase activity in samples treated with E7386 to that in samples not treated with E7386 (control). IC_{50} values were calculated by using Prism Software (version 8.0.1, GraphPad Software).

In vivo antitumor activity

All animal experiments in this study were conducted in accordance with the guidelines for animal experiments of Eisai Co., Ltd. ECC10 cells were injected subcutaneously into the right flank of female nude mice (CAnN.Cg-Foxn1nu/Crl; Charles River Laboratories Japan) and tumors were allowed to grow to 150–200 mm^3 in size (designated day 1). MMTV-Wnt1 transgenic mice [B6SJL-Tg(Wnt1)1Hev/J] were obtained from the Jackson Laboratory. Spontaneously developed breast tumors were resected from the MMTV-Wnt1 transgenic mice, diced, and inoculated into C57BL/6J mice (Charles River Laboratories Japan). Tumors were allowed to grow to approximately between 80 and 200 mm^3 in size (designated day 1); tumor-bearing mice were then randomly allocated to treatment groups and orally administered with E7386 (12.5, 25, or 50 mg/kg twice daily) or intraperitoneally administered with anti-PD-1 antibody (500 μg/mouse twice weekly). Tumor sizes were measured with digital calipers, and tumor volumes were calculated as long length × short length^2 × 0.5. Statistical analyses were performed by using Prism software.

Intestinal polyp formation in the $Apc^{Min/+}$ mouse model

$Apc^{Min/+}$ mice, which harbor a truncating nonsense mutation at codon 850 of the *Apc* gene, developed a spontaneous intestinal

adenoma (25, 26). Four-week-old $Apc^{Min/+}$ mice (C57BL/6J-Apc^{Min}/J) were orally administered 10 cycles of E7386 (6.25–50 mg/kg twice daily) according to a schedule of 5 days on/2 days off. After treatment, the mice were euthanized, and the polyps in the small intestine were counted under a stereo microscope. Eight-week-old $Apc^{Min/+}$ mice were orally administered four cycles of E7386 (30 mg/kg twice daily) according to a same schedule. After the final administration, samples of small intestine and whisker follicles were collected.

Microarray analysis

Total RNA was extracted from the whisker follicles of $Apc^{Min/+}$ mice by using an RNeasy Kit (Qiagen). An aliquot of total RNA (50 ng) was converted to cyanine-3–labeled cRNA by using a Low Input Quick Amp Labeling Kit, One-Color, and then hybridized to a SurePrint G3 Mouse GE 8 × 60K Microarray (Agilent Technologies). Hybridization images were obtained with a DNA Microarray Scanner (Agilent Technologies) and quantified by using Feature Extraction Software (version 11, Agilent Technologies). Raw data were normalized by using the quantile function in R software (version 3.1.0). *P* values were determined by using Welch *t* test, followed by adjustment for multiple comparisons by using an FDR approach (Benjamini–Hochberg procedure) in R software (version 3.1.0). A gene was considered differentially expressed when its absolute fold change relative to the control value was ≥2 and it had an FDR $P < 0.05$. Pathway analysis was conducted by using the Ingenuity Pathway Analysis Platform (Qiagen). The microarray data have been deposited in the NCBI Gene Expression Omnibus under accession number GSE158554.

nCounter gene expression analysis

Total RNA was extracted from ECC10 tumor tissues from mice treated with either vehicle or E7386 (12.5, 25, or 50 mg/kg) and analyzed by using an nCounter Vantage 3D RNA Wnt Pathways Panel (NanoString Technologies). Data were imported into nSolver analysis software (version 4.0) to check the quality, and then normalized on the basis of positive probes and housekeeping genes. Differentially expressed genes (DEG) were identified for each E7386 dose group compared with vehicle by using the following criteria: |fold change| > 1.25 and $P < 0.1$ (Welch *t* test). The $\log_2$ ratios of DEGs identified in at least one dose group were visualized as a heatmap by using Strand NGS Software (Agilent Technologies).

RNA sequencing analysis

Total RNA was extracted from MMTV-Wnt1 tumor tissues resected from mice treated with either vehicle or E7386 at 3 (day 4) and 7 days (day 8) after initiation of each treatment and used for RNA sequencing (RNA-seq) analysis. Sequencing libraries were generated from isolated RNA by using an Illumina TruSeq mRNA Library Kit according to the manufacturer's instructions. Paired-end sequencing of 2 × 150 bp was conducted by using an Illumina NextSeq 500 in accordance with the manufacturer's instructions. FastQ files for each sample converted from the binary base call file were entered into FastQC (http://www.bioinformatics.babraham.ac.uk/projects/fastqc/) for quality assessment. Sequencing data were processed by using Trimmomatic (version 0.36; ref. 27) to remove all Illumina adaptor sequences and bases with low quality scores. Filtered reads were mapped to the mouse genome (Mm10 and Ensembl 84) by using STAR software (version 2.5.0c; ref. 28). Gene expression levels, in transcripts per million, were estimated for all samples by using RSEM software (version 1.2.31; ref. 29). The RNA-seq data have been deposited in the NCBI Gene Expression Omnibus under accession number GSE158713.

Gene expression profiling analysis using RNA-seq data

Differential gene expression analysis was performed at Clarivate Analytics by using the DESeq2 R package (30). The most relevant metrics were the fold change in expression relative to the vehicle group, the raw *P* value derived from the statistical test, and the *P* value adjusted for multiple comparisons according to Benjamini–Hochberg correction. Topologically significant genes (TS genes) were identified by using four methods: overconnectivity, interconnectivity, network propagation, and causal reasoning (31–35). All of these methods were used for the input; the lists of DEGs were derived from each E7386 dose group compared with vehicle, after splitting genes into those that were downregulated and those that were upregulated. Enrichment analysis using DEGs, TS genes, and the nonredundant union of both gene lists was performed against pathway maps obtained from Metabase at Clarivate Analytics. Cell type deconvolution analysis was performed by using the CIBERSORT algorithm (36), which uses gene expression data to provide an estimation of the abundances of cell types in a mixed cell population.

IHC

MMTV-Wnt1 tumor tissues were resected from mice orally administered with 50 mg/kg of E7386 twice daily for a week. Fresh frozen tumor tissues were embedded in Optimal Cutting Temperature Compound (Sakura Finetek) and cut into 10-μm-thick sections. Staining was performed by using anti-CD8 antibody (clone 53-6.7, 1:100, eBioscience) in combination with Alexa Fluor 594–conjugated donkey anti-rat IgG (1:100, Life Technologies), with DAPI (4′,6-diamidino-2-phenylindole, Dojindo) as the counterstain. The sections were scanned by using a White-light Confocal Microscope (Leica Microsystems, TCS SP8), and the $CD8^+$ cells within tumors were counted in a blinded manner by using scanned images at 200× magnification.

Results

Blockade of the β-catenin/CBP interaction by E7386

First, we investigated that E7386 (**Fig. 1A**) blocked the interaction between the exogenous N-terminal region of CBP and endogenous β-catenin in HEK293 cells overexpressing FLAG-tagged N-terminal region of CBP, and we also examined those reported for ICG-001, the first-reported inhibitor of the β-catenin–CBP interaction (24), and C-82 (**Fig. 1A**). HEK293 cells were incubated with 40 mmol/L LiCl to inhibit the phosphorylation of β-catenin by GSK3β and activate the Wnt/β-catenin signaling pathway (i.e., induce the interaction between β-catenin and CBP). Coimmunoprecipitation of β-catenin and anti-FLAG antibody from whole-cell lysate was markedly decreased in cells treated at the highest dose for each of the test compounds, indicating that all of the compounds decreased the interaction between β-catenin and CBP (**Fig. 1B**). On the other hand, coimmunoprecipitation of β-catenin and anti-FLAG antibody was decreased when the lowest dose of E7386 (0.5 μmol/L) was used.

Next, we examined whether E7386 inhibited the interaction of endogenous β-catenin and CBP by using *APC*-mutated human gastric cancer ECC10 cells, in which the Wnt/β-catenin signaling pathway is highly activated (Supplementary Fig. S1). ECC10 cells were treated with E7386 or ICG-001 for 6 hours, and CBPs in the cell lysate were coimmunoprecipitated with anti-CBP antibody. The amount of β-catenin bound to CBP was determined by Western blotting. E7386 decreased the interaction between β-catenin and CBP in a dose-dependent manner (**Fig. 1C**). However, neither of the test compounds interfered with the interaction between β-catenin and p300 (Supplementary Fig. S2).

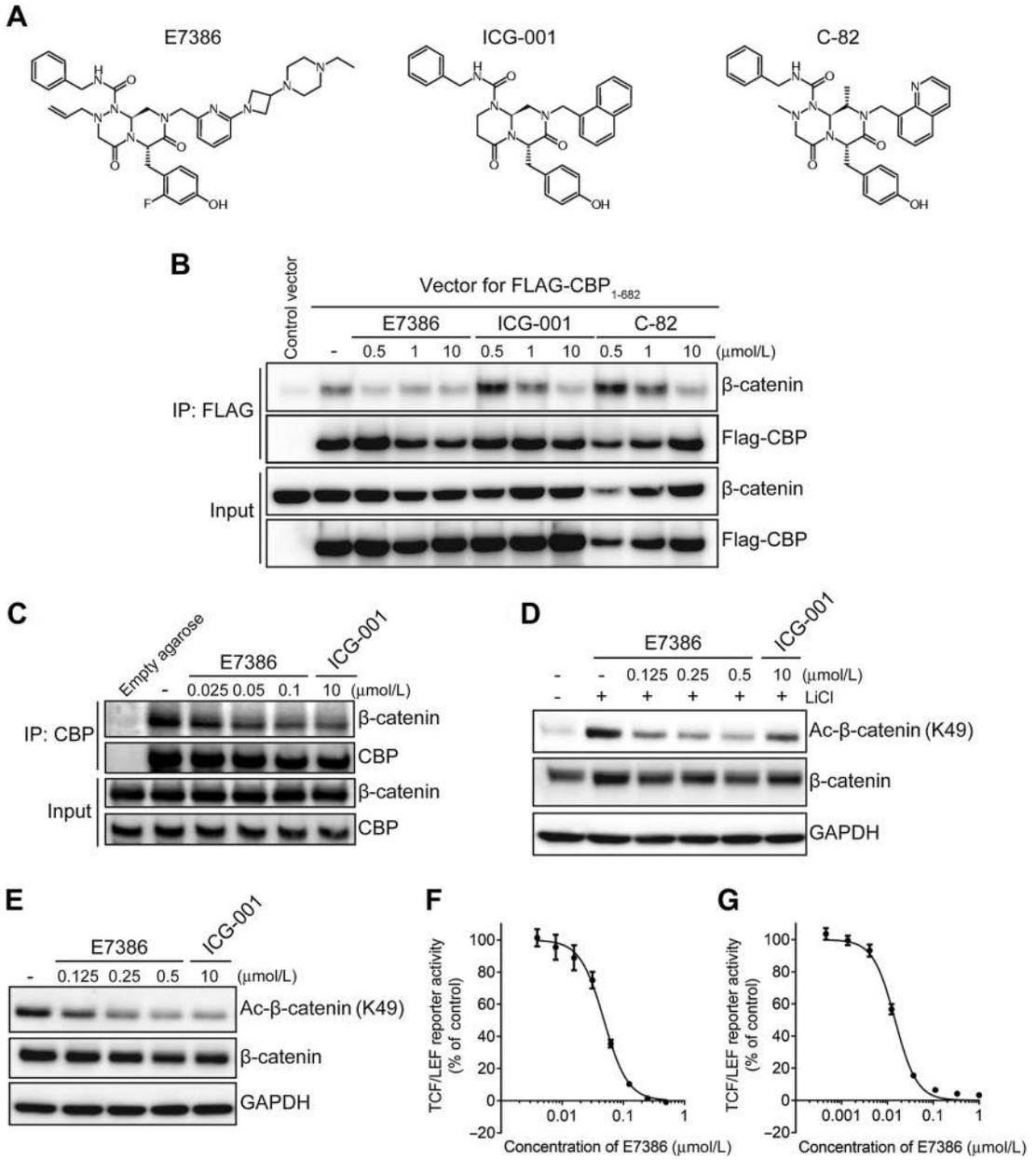

Figure 1.

Blockade of the β-catenin/CBP signaling pathway by E7386. **A,** Chemical structure of E7386 (left), ICG-001 (middle), and C-82 (right). **B** and **C,** Blockade of the interaction of β-catenin with CBP. Whole-cell lysates were loaded to the gel without immunoprecipitations (IP; input). **B,** HEK293 cells overexpressing FLAG-tagged N-terminal region of CBP were stimulated with LiCl and then treated with E7386, ICG-001, or C-82. At 6 hours after treatment, whole-cell extracts were coimmunoprecipitated with anti-FLAG affinity gels and immunoblotted with anti-β-catenin or anti-FLAG antibody. **C,** ECC10 cells were treated with 0.025–0.1 μmol/L of E7386 or 10 μmol/L of ICG-001. At 6 hours after treatment, whole-cell extracts were incubated with anti-CBP antibody immobilized on agarose or with empty agarose and then immunoblotted with anti-β-catenin and anti-CBP antibodies. **D** and **E,** Western blot analysis of acetylated (Ac) β-catenin. LiCl-stimulated HEK293 (**D**) and ECC10 (**E**) cells were treated for 2 hours with E7386 or ICG-001 at the indicated concentrations. Whole-cell extracts were immunoblotted with anti-acetyl β-catenin, anti-β-catenin, or anti-GAPDH antibodies. **F** and **G,** TCF/LEF reporter assay. **F,** HEK293 cells stably expressing TCF/LEF reporter were incubated in medium containing 40 mmol/L LiCl and then treated with or without E7386. Luciferase activity was determined at 6 hours after E7386 treatment. **G,** ECC10 cells were transfected with TCF/LEF reporter plasmid, and after 48 hours, the cells were incubated with E7386 for 6 hours. Luciferase activity was determined at 6 hours after E7386 treatment. Data are shown as means ± SEM ($n = 3$).

CBP has intrinsic acetyltransferase activity against lysine 49 of β-catenin (37). Therefore, we also examined whether inhibition of the interaction of β-catenin with CBP by E7386 affected acetylation of lysine 49 (**Fig. 1D** and **E**). E7386 clearly decreased the acetylation of lysine 49 of β-catenin in both HEK293 and ECC10 cells.

Blockade of the β-catenin/CBP signaling pathway by E7386

Upon activation of the Wnt/β-catenin signaling pathway, β-catenin enters the nucleus where it engages with DNA-bound TCF transcription factors. Thus, reporter assays using the TCF/LEF binding motif, such as the TOPFlash assay, can be used to examine activation of the Wnt/β-catenin signaling pathway (1). To assess the effect of inhibition of β-catenin and CBP interaction by E7386 on the Wnt/β-catenin signaling pathway, we investigated the effect of E7386 on the Wnt/β-catenin signaling pathway by using a TCF/LEF reporter assay using HEK293 cells stably expressing TCF/LEF luciferase reporter and ECC10 cells transfected with an expression vector for TCF/LEF luciferase reporter (**Fig. 1F** and **G**). E7386 treatment for 6 hours inhibited TCF/LEF luciferase activity in a dose-dependent manner in both cell lines. The IC_{50} value of E7386 in HEK293 and ECC10 cells was 0.0484 and 0.0147 μmol/L, respectively.

We also investigated the effects of ICG-001 and C-82 by using the same TCF/LEF reporter assay (Supplementary Fig. S3A). In HEK293 cells stimulated with LiCl, ICG-001 and C-82 both disrupted TCF/LEF reporter activity in a dose-dependent manner (IC_{50} values, 3.31 and 0.356 μmol/L, respectively; Supplementary Fig. S3B). Thus, in this assay, the effect of E7386 against the Wnt/β-catenin signaling pathway in HEK293 cells (IC_{50} value, 0.0484 μmol/L) was stronger than that of ICG-001 and C-82.

Inhibitory activity of E7386 against polyp formation in *Apc*$^{Min/+}$ mice

Apc$^{Min/+}$ mice (C57BL/6J-*Apc*^{Min}/J) are genetically engineered with a truncating mutation in the *Apc* gene, which causes them to spontaneously develop intestinal adenomas due to aberrant activation of the Wnt/β-catenin signaling pathway (25, 26). *Apc*$^{Min/+}$ mice were administered with E7386 (6.25–50 mg/kg orally, twice daily) for 10 cycles (each cycle, 5 days on/2 days off) from 4 weeks of age. After the 10 cycles of treatment, the polyps that formed in the small intestine were counted (**Fig. 2A**). The number of polyps was 10 times higher in 14-week-old mice than in 4-week-old mice in the vehicle group, and administration of E7386 significantly suppressed polyp formation in a dose-dependent manner compared with the vehicle group (**Fig. 2B**). Relative body weights on the final day (i.e., ratio of body weight at day 71 to that at day 1) were 1.33 (vehicle), 1.33 (E7386, 6.25 mg/kg), 1.30 (12.5 mg/kg), 1.26 (25 mg/kg), and 1.19 (50 mg/kg). Thus, no marked loss of body weight was observed at any of the doses examined.

The Wnt/β-catenin signaling pathway is reported to be activated in hair and whisker follicles (38, 39). In humans, pre- and posttreatment hair follicles from patients treated with ipafricept, which is a truncated Fzd8 receptor fused to the Fc region of IgG1, showed suppression of Wnt/β-catenin–dependent genes (18). Thus, we next examined whether E7386 disrupted the Wnt/β-catenin signaling pathway by using whisker follicles of *Apc*$^{Min/+}$ mice. E7386 (30 mg/kg orally, twice daily) was administered for four cycles (each cycle, 5 days on/2 days off) from 8 weeks of age. Small intestines and whisker follicles were collected at 6 hours after the final administration. E7386 significantly decreased the number of polyps compared with the vehicle group (Supplementary Fig. S4A). Microarray analysis of total RNA extracted from the whisker follicles of mice treated with E7386 revealed that 183 genes were differentially expressed compared with vehicle treatment ($|\text{fold change}| \geq 2$; $P < 0.05$). Subsequent pathway analysis using the ingenuity pathway analysis platform identified WNT3A as the upstream regulator with highest *P* value of overlap (activation z-score, −2.4; $P = 1.77 \times 10^{-5}$), indicating that the canonical Wnt/β-catenin signaling pathway was disrupted by E7386 in the whisker follicles of *Apc*$^{Min/+}$ mice (Supplementary Fig. S4B).

Antitumor activity of E7386 in the human gastric cancer ECC10 xenograft model

E7386 significantly suppressed the growth of ECC10 cells *in vitro* (IC_{50} value, 4.9 nmol/L) and induced a cell death in cells exposed to concentrations ≥10 nmol/L for 7 days (Supplementary Fig. S5). This suggested that the proliferation and survival of ECC10 cells are dependent on the Wnt/β-catenin signaling pathway. We, therefore, conducted an *in vivo* study to examine the antitumor activity of E7386 in the ECC10 tumor xenograft model. ECC10 cells were subcutaneously inoculated into mice, and when the tumor size reached 150 mm^3 (designated day 1), the mice were randomly allocated to groups treated with vehicle or E7386 at 12.5, 25, or 50 mg/kg orally, twice daily for 7 days. E7386 showed *in vivo* antitumor activity in a dose-dependent manner, and significantly inhibited tumor growth when administered at 25 or 50 mg/kg (**Fig. 3A**) without any significant changes in body weight (**Fig. 3B**). E7386 treatment for 14 days at 12.5, 25, or 50 mg/kg also showed significant dose-dependent antitumor activity *in vivo* without any significant changes in body weight (Supplementary Fig. S6A). In contrast, 100 mg/kg of ICG-001 showed only slight antitumor activity and this observation was not statistically significant (Supplementary Fig. S6B).

We then analyzed the expression profile of genes related to the Wnt/β-catenin signaling pathway by using the nCounter analysis platform (**Fig. 3C**). Gene expression analysis revealed that seven, six, and 41 genes related to the Wnt/β-catenin signaling pathway were differentially expressed in ECC10 tumor tissues resected from mice treated with E7386 at 12.5, 25, or 50 mg/kg, respectively, compared with vehicle treatment ($|\text{fold change}| > 1.25$; $P < 0.1$; Supplementary Table S1). At 50 mg/kg, E7386 upregulated 19 genes and downregulated 22 genes related to the Wnt/β-catenin signaling pathway. Of the well-known downstream genes of the Wnt/β-catenin signaling pathway, *PTGS2* and *CCND1* were significantly downregulated and *WISP1* was significantly upregulated (**Fig. 3C**; Supplementary Table S1; refs. 40–42). Collectively, these data suggested that modulation of Wnt/β-catenin signaling pathway by E7386 led to antitumor activity in tumor models showing activated Wnt/β-catenin signaling pathway.

Antitumor activity of E7386 in the MMTV-Wnt1 mouse breast tumor model

We evaluated the antitumor activity of E7386 in the MMTV-Wnt1 isogenic mouse breast tumor model, in which tumor cells were originated from breast epithelial cells by the Wnt/β-catenin signaling pathway activated by overexpression of Wnt1 under an immunocompetent tumor microenvironment (43). C57BL/6J mice bearing MMTV-Wnt1 tumors, which had been inoculated using diced tumor tissues developed in MMTV-Wnt1 mice, were randomly assigned to treatment groups at 14 days after transplantation, when average tumor sizes reached 220 mm^3 (designated day 1), and then E7386 at 12.5–50 mg/kg was orally administered twice daily for 7 days. E7386 significantly inhibited tumor growth in a dose-dependent manner without marked body weight loss (**Fig. 4A** and **B**).

Next, we conducted an RNA-seq analysis using total RNA extracted from MMTV-Wnt1 tumor tissues resected from mice orally

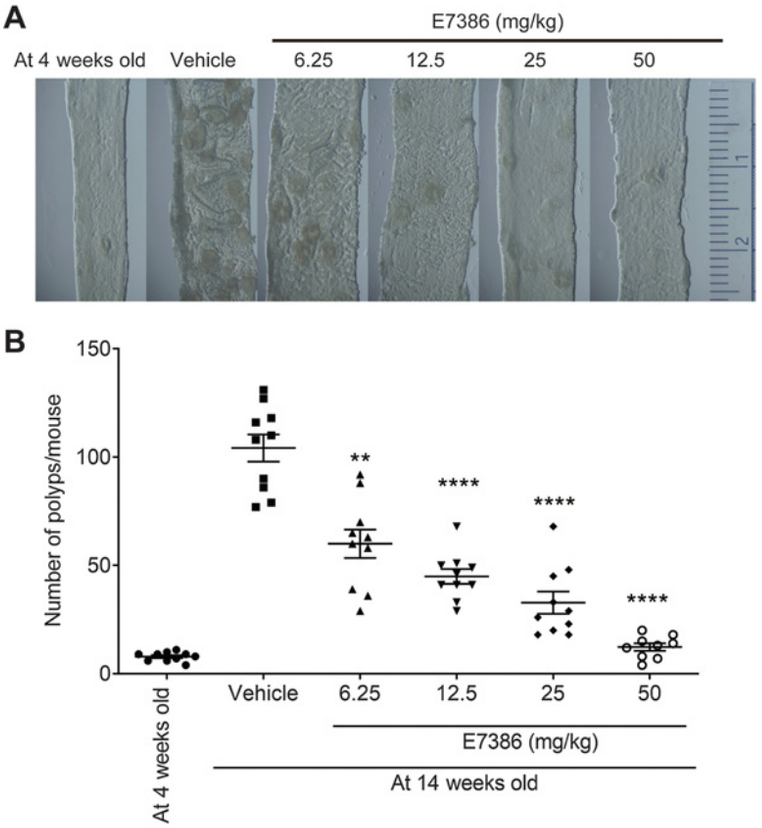

Figure 2.

Effect of E7386 on spontaneous intestinal polyp formation in $Apc^{Min/+}$ mice. E7386 was orally administered to $Apc^{Min/+}$ mice (4 weeks old) at 6.25–50 mg/kg twice daily for 10 cycles (each cycle, 5 days on/2 days off). After treatment, the mice were euthanized, and the polyps in the small intestine were counted. **A,** Macroscopic photographs of the intestine of a representative mouse from each group. **B,** Number of polyps per mouse (means ± SEM; $n = 10$). The number of polyps was significantly decreased (**, $P < 0.01$; ****, $P < 0.0001$ by Dunnett test) in all treatment groups compared with vehicle.

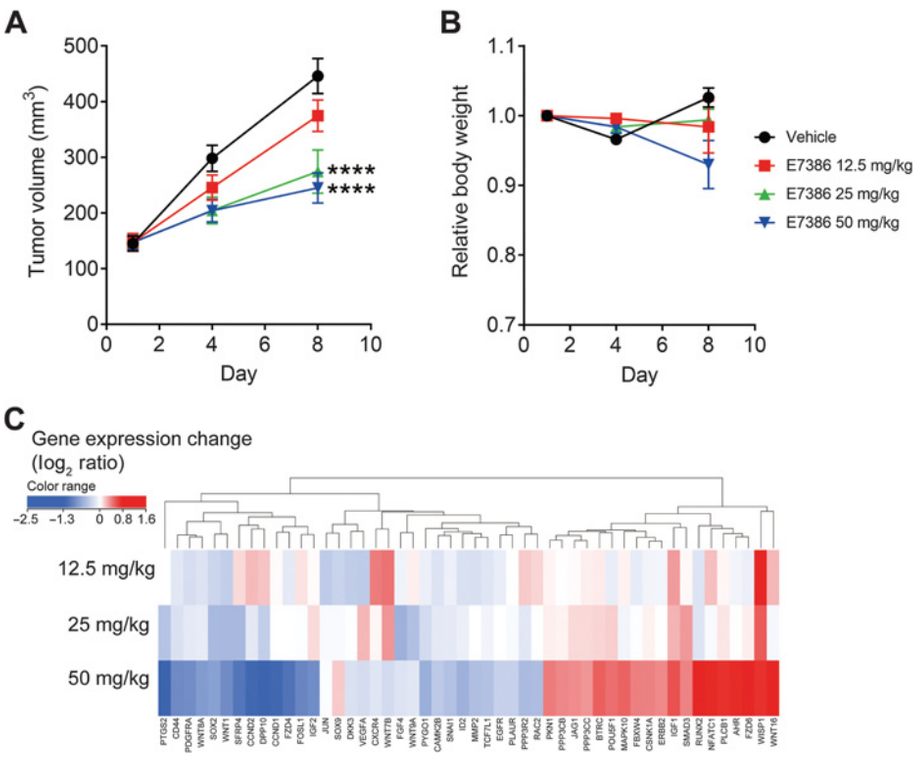

Figure 3.

Antitumor activity of E7386 and gene expression profile analysis in the human ECC10 gastric tumor xenograft model. ECC10 cells were subcutaneously inoculated into female nude mice. When the mean tumor volume reached 150 mm^3 (designated day 1), the mice were orally administered with vehicle or E7386 at 12.5–50 mg/kg twice daily for 7 days. **A** and **B,** Tumor volume (**A**) and relative body weight (**B**) were measured at indicated days; data are shown as means ± SEM ($n = 5$). ****, $P < 0.0001$ versus vehicle by repeated measures ANOVA, followed by Dunnett test for multiple comparisons. **C,** The heatmap showing log_2-fold changes of DEGs between treatment and vehicle groups (|fold change| > 1.25; $P < 0.1$). At day 7, tumors were collected, total RNA was extracted, and the expressions of genes in Wnt/β-catenin signaling pathway were examined.

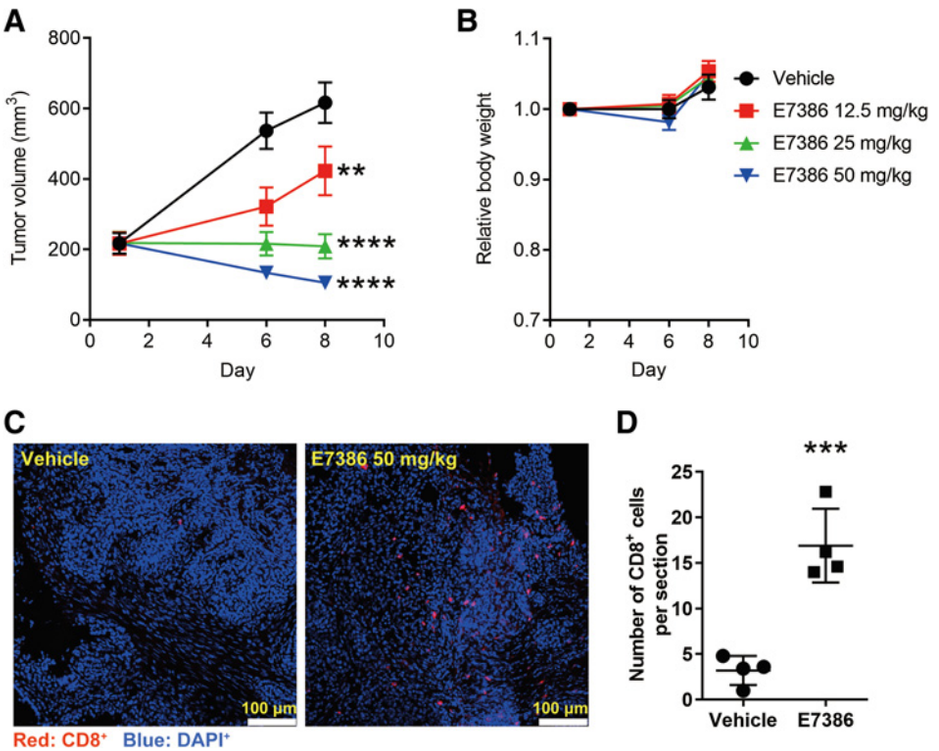

Figure 4.

Antitumor activity and immunomodulatory effect of E7386 in the MMTV-Wnt1 mouse breast tumor model. Tumors growing in MMTV-Wnt1 mice were collected, diced, and then inoculated into C57BL/6J mice to afford an isogenic mouse tumor model. The mice were orally administered with E7386 at 12.5–50 mg/kg twice daily, or vehicle, for 7 days. **A** and **B,** Tumor volume (**A**) and relative body weight (**B**) were measured at indicated days; data are shown as means ± SEM ($n = 5$). **, $P < 0.001$; ****, $P < 0.0001$ versus vehicle by repeated measures ANOVA, followed by Dunnett test for multiple comparisons. **C,** Representative images of CD8 staining in tumor tissues. Red, CD8-positive cell; blue, DAPI-positive cell. **D,** Number of $CD8^+$ cells per tumor cross-section (0.34 mm^2). ***, $P < 0.001$ by unpaired *t* test versus vehicle.

administered with E7386 at 25 or 50 mg/kg twice daily, or vehicle, for 3 (day 4) or 7 days (day 8) and examined the DEG levels compared with vehicle at days 4 and 8. We observed a higher number of DEGs with $P < 0.05$ when E7386 was administered at 50 mg/kg (1,363 and 722 at days 4 and 8, respectively) than when it was administered at 25 mg/kg (801 and 501 at days 4 and 8, respectively; Supplementary Table S2). We also identified key regulators, TS genes, of the expression of DEGs by using four methods: overconnectivity, interconnectivity, network propagation, and causal reasoning in the list of DEGs (Supplementary Table S3; refs. 31–35).

We next searched for functional ontologies that were enriched in the list of DEGs and the result of a nonredundant union of both gene lists using pathway maps in Metabase (Supplementary Table S4). The top 10 results of the pathway map analysis at 50 mg/kg on day 8 using the downregulated gene set data revealed that immune-related and hypoxia-related genes were significantly downregulated (**Table 1**). Among these gene sets, "transcription_HIF-1 targets" and "immune responses_CCL2 signaling" were detected for both the 25 and 50 mg/kg doses with a significant *P* value. In addition, signaling pathways regulating the tumor microenvironment, including genes related to the innate immune response to contact with allergens or the $CD8^+$ Tc1 cell (i.e., cytotoxic T cell) pathway, were significantly upregulated when E7386 was administered at 50 mg/kg (**Table 1**). These results suggested that E7386 treatment for 7 days altered the tumor microenvironment and immune cell population in tumors.

We next applied the immune cell type deconvolution algorithm CIBERSORT (36) to the RNA-seq data to examine how E7386 affected immune cell populations in tumor tissues (Supplementary Table S5). Twenty-five immune cell subtypes were identified in MMTV-Wnt1 tumor tissues. Among them, monocytes, M2 macrophages, and activated dendritic cells (DC) were decreased, and M0 and M1 macrophages, immature DCs, and $CD4^+$ naïve T cells were increased compared with vehicle at day 8 in mice treated with E7386 at 50 mg/kg.

From an IHC analysis, Spranger and colleagues have reported an inverse association between stabilized β-catenin and $CD8^+$ T cells in clinical tumor samples (14), suggesting that activation of the Wnt/β-catenin signaling pathway suppressed the infiltration of lymphocytes into tumor. To examine whether disruption of the Wnt/β-catenin signaling pathway by E7386 leads to an increase of $CD8^+$ T cells, we further investigated the effect of E7386 on immune activation, $CD8^+$ cells in tumor tissue were stained with anti-CD8 antibody and analyzed by fluorescence IHC (**Fig. 4C** and **D**); the number of $CD8^+$ cells was increased in tumor tissues resected from mice treated with E7386 at 50 mg/kg compared with that in mice treated with vehicle.

Synergistic antitumor activity of E7386 and anti-PD-1 antibody in the MMTV-Wnt1 mouse tumor model

β-catenin activation promotes immune escape and resistance to anti-PD-1 therapy (15). To investigate whether the immunomodulatory effect of E7386 is related to its antitumor effect, we tested the antitumor activity of E7386 in combination with anti-PD-1 antibody in a Wnt/β-catenin signaling pathway–activated syngeneic mouse model, the MMTV-Wnt1 mouse breast tumor model. C57BL/6J mice bearing MMTV-Wnt1 tumors were assigned to treatment groups at 14 days after transplantation of MMTV-Wnt1 tumor fragments (designated day 1; when the average tumor size had reached ~80 mm^3), and then treated with E7386 at 50 mg/kg orally, twice daily, anti-PD-1 antibody at 500 μg/mouse intraperitoneally, twice weekly for 21 days, or a combination of both. Anti-PD-1 antibody alone showed no antitumor activity, and E7386 alone showed slow-growing tumors. However, combination treatment of E7386 with anti-PD-1 antibody significantly enhanced the antitumor activity of E7386 (**Fig. 5A** and **B**). No severe loss of body weight was observed, indicating that the combination treatment was as tolerable as the monotherapy (**Fig. 5C**).

Table 1. Top 10 signaling pathways affected by E7386 in the MMTV-Wnt1 mouse breast tumor model.

DEG category (downregulated genes at day 8)	25 mg/kg *P* (log_{10})	50 mg/kg *P* (log_{10})
Transcription_HIF-1 targets	−8.42	−42.55
Immune response_C5a signaling	−10.40	−19.24
Stem cells_endothelial differentiation during embryonic development	N.S.	−18.65
Regulation and signaling of HGF receptor and MSP receptor in lung cancer	N.S.	−18.61
Immune response_CCL2 signaling	−14.43	−18.24
HIF-1 in gastric cancer	N.S.	−18.02
Role of alpha-V/beta-6 integrin in colorectal cancer	N.S.	−16.72
Role of adipose tissue hypoxia in obesity and type 2 diabetes	N.S.	−15.94
Development_PIP3 signaling in cardiac myocytes	N.S.	−15.44
Transport_Alpha-2 adrenergic receptor regulation of ion channels	N.S.	−14.55

DEG category (upregulated genes at day 8)	25 mg/kg *P* (log_{10})	50 mg/kg *P* (log_{10})
SLE genetic marker–specific pathways in B cells	N.S.	−11.66
Development_NOTCH-induced EMT	N.S.	−10.96
The innate immune response to contact allergens	N.S.	−8.69
Cytoskeleton remodeling_keratin filaments	N.S.	−8.08
The role of KEAP1/NRF2 pathway in skin sensitization	N.S.	−7.74
Cornification of epithelium in dry eye	N.S.	−6.78
Development_keratinocyte differentiation	N.S.	−5.51
Stem cells_H3K36 demethylation in stem cell maintenance	N.S.	−4.86
Prooncogenic action of androgen receptor in breast cancer	N.S.	−3.50
$CD8^+$ Tc1 cells in allergic contact dermatitis	N.S.	−3.42

Note: MMTV-Wnt1 tumors were collected 7 days (day 8) after treatment with E7386, and total RNA was subjected to RNA-seq analysis. The top 10 results of the pathway map on day 8 using the nonredundant union lists are shown.
Abbreviation: N.S., not significant.

Next, we used flow cytometry to investigate the effect of E7386 and combination treatment of E7386 plus anti-PD-1 antibody on the immune cell populations in MMTV-Wnt1 tumors. Immune cell populations were determined by using antibodies listed in Supplementary Table S6, and the gating strategy shown in Supplementary Fig. S7. Among the myeloid populations, both E7386 treatment alone and the combination treatment significantly decreased the M2 macrophage population, gated as $CD11b^+F4/80^+Ly6C^{low}I\text{-}A/I\text{-}E^{low}C\text{-}D86^{low}$, and significantly increased the M1/M2 macrophage ratio (Supplementary Fig. S8A–S8D). The $CD8^+$ T-cell population tended to be increased by combination treatment compared with vehicle, although this change was not statistically significant. However, the $CD8^+$ T-cell/$CD4^+$ T-cell ratio was significantly increased by both anti-PD-1 antibody treatment alone and the combination treatment compared with vehicle (Supplementary Fig. S8E–S8H). Consistent with our CIBERSORT findings, $CD8^+$ T cells in MMTV-Wnt1 tumor were upregulated by combination treatment accompanied by a decrease of M2 macrophages and increase of the M1/M2 ratio.

Collectively, these data indicated that E7386 showed synergistic combination antitumor activity with anti-PD-1 antibody in the MMTV-Wnt1 model.

Discussion

Here, we found that E7386 inhibited the interaction between β-catenin and CBP *in vitro* and that orally administered E7386 inhibited the development of adenoma polyps in $Apc^{Min/+}$ mice. *In vivo*, E7386 inhibited the growth of ECC10 human xenografted tumors in nude mice, as well as the growth of MMTV-Wnt1 mouse breast tumors in immunocompetent mice with induction of tumor-infiltrating lymphocyte. Moreover, E7386 exhibited synergistic antitumor activity in combination with anti-PD-1 antibody in a MMTV-Wnt1 mouse tumor model.

The effect of E7386 against the Wnt/β-catenin signaling pathway was more potent than the activities of ICG-001 and C-82, which are previously reported inhibitors of the β-catenin/CBP interaction (**Fig. 1**; Supplementary Fig. S3). Oral administration of E7386 at 6.25 mg/kg suppressed intestinal polyp formation in $Apc^{Min/+}$ mice, whereas PRI-724 at 300 mg/kg was required to achieve comparable inhibition (Supplementary Fig. S9). Because E7386 has 80-fold metabolic stability compared with C-82 (Supplementary Table S7), it may contribute to lower doses of E7386 to show inhibitory activity in addition to the intrinsic potent activity of E7386 compared with PRI-724.

In vitro, E7386 inhibited the growth of ECC10 cells at concentrations near the Wnt/β-catenin signaling pathway (**Fig. 1G**; Supplementary Fig. S5). These results suggest that the proliferation of ECC10 cells is dependent on the Wnt/β-catenin pathway and that E7386 inhibits cell growth by modulating Wnt/β-catenin signaling. The clear antitumor activity of E7386 in the ECC10 xenograft model (**Fig. 3**) and the findings of the DEGs analysis of ECC10 tumors were consistent with this hypothesis. In the DEGs analysis of genes related to the Wnt/β-catenin signaling pathway in the ECC10 tumor xenograft model, E7386 was found to decrease the expression of *CCND1* and increase the expression of *WISP1* (Supplementary Table S1). It has been reported that CBP occupies the *CCND1* promoter and that ICG-001 inhibits the occupancy of this site by CBP (24). *WISP1* is reported to be a β-catenin/p300 target gene (44). These previous reports suggest that E7386-mediated modulation of Wnt/β-catenin downstream genes in ECC10 tumor cells results in selective inhibition of the interaction between β-catenin and CBP. Emami and colleagues have shown that

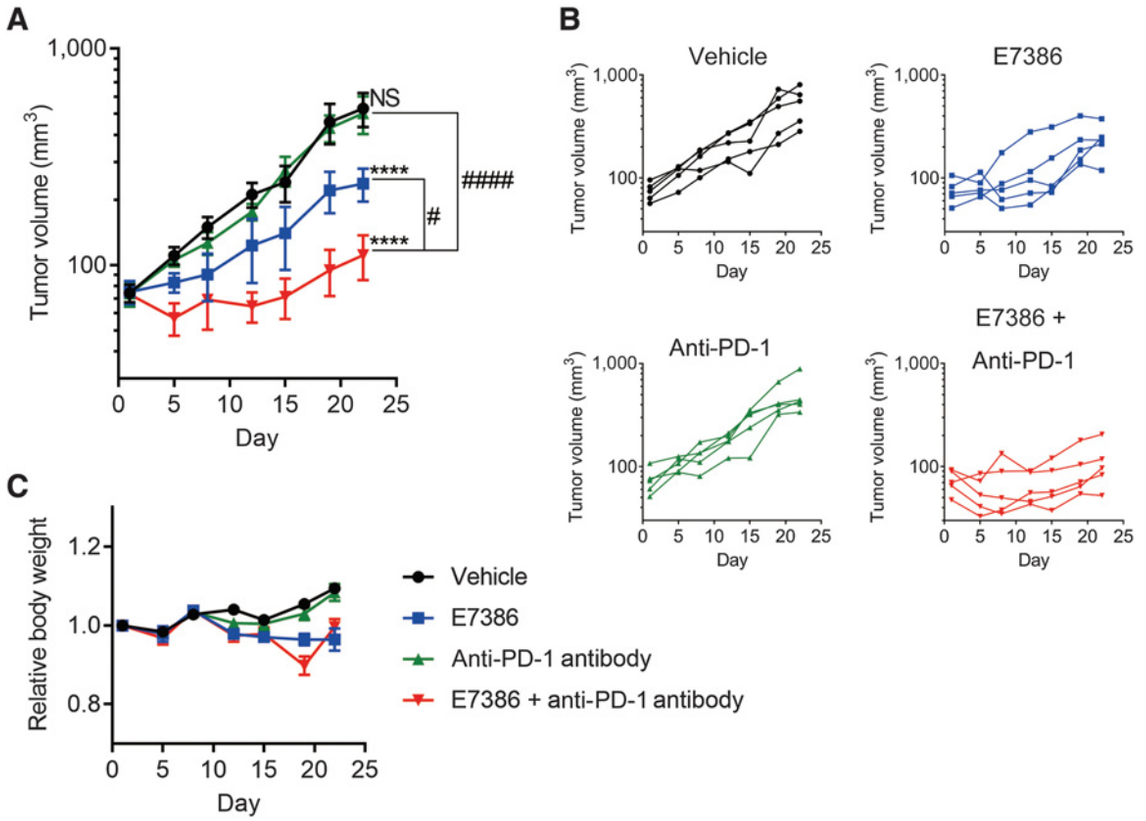

Figure 5.

Antitumor activity of E7386 in combination with anti-PD-1 antibody in the MMTV-Wnt1 mouse breast tumor model. Tumors growing in MMTV-Wnt1 transgenic mice were collected, diced, and inoculated into C57BL/6J mice to afford the isogenic mouse MMTV-Wnt1 tumor model. When tumor volumes reached an average of approximately 80 mm^3, the mice were orally treated with either vehicle, 50 mg/kg of E7386 twice daily, 500 μg/mouse of anti-PD-1 antibody twice weekly intraperitoneally, or a combination of E7386 and anti-PD-1 antibody for 21 days. **A,** Tumor volumes were measured at indicated days. **B,** Tumor volumes for individual mice are shown for each treatment group. **C,** Relative body weight measurements during the treatment. Data are shown as means ± SEM ($n = 5$). ****, $P < 0.0001$ or NS, not significant, versus vehicle; #, $P < 0.05$; ####, $P < 0.0001$ versus combination by repeated measures ANOVA, followed by Dunnett test for multiple comparisons.

ICG-001, previously reported analogue compound of E7386, binds to amino acids 1–111 of CBP, and that the complex between these amino acids and β-catenin is inhibited by treatment with ICG-001 (24). In contrast, they have also shown that ICG-001 does not inhibit the binding of β-catenin to amino acids 1 through 111 of p300. Together with our data showing that E7386 blocks the interaction between β-catenin and CBP, but not between β-catenin and p300, these findings suggest that the activity of E7386 is likely due to an increase in the binding of β-catenin with p300.

In our RNA-seq analysis using the MMTV-Wnt1 mouse breast tumor model, signaling pathways related to immunity and inflammation, such as "immune response_CCL2 signaling," were downregulated at day 8 in animals administered with E7386 at 25 and 50 mg/kg. In addition, a signaling pathway related to hypoxia was significantly downregulated at days 4 and 8 when E7386 was administered at 25 mg/kg (**Table 1**; Supplementary Table S4). It has been reported that CCL2 and hypoxia signals play important roles in immune resistance and suppression of immune status by tumor microenvironments (45, 46). From our results, it was hypothesized that E7386 altered the immunosuppressive tumor microenvironment by modulation of the Wnt/β-catenin signaling pathway.

Consistent with the findings of our DEGs analysis, immune deconvolution analysis revealed that E7386 altered immune cell populations by increasing the immunostimulatory macrophage population (i.e., M1 macrophages) and decreasing the immunosuppressive macrophage population (i.e., M2 macrophages), resulting in an increase in the M1/M2 macrophage ratio. It has been reported that activation of the Wnt/β-catenin signaling pathway promotes M2 macrophage polarization, and that knockdown of Wnt ligand inhibits tumor growth in association with a decrease in the M2 macrophage population and an increase in the cytotoxic T lymphocyte population (47). In addition, CCL2 is a key chemokine for polarizing macrophages toward M2 macrophages (48). In this study, we found that E7386 increased the number of $CD8^+$ cells in MMTV-Wnt1 tumor tissue (**Fig. 4C**). Together, these findings suggest that E7386-mediated modulation of the Wnt/β-catenin signaling pathway decreases M2 macrophages and increases tumor-infiltrating $CD8^+$ cells.

Lymphocyte infiltration and an IFNγ signature define the T-cell–inflamed tumor phenotype (referred to as "hot tumor"), and their presence is essential for anti-PD-1 antibody therapy to be effective. In contrast, "cold tumors" lack lymphocyte infiltration and an IFNγ signature and are resistant to anti-PD-1 antibody therapy (49, 50). Activation of the Wnt/β-catenin signaling pathway in the tumor

microenvironment causes T-cell exclusion. Wnt/β-catenin signal–activated murine melanoma shows impaired priming of antitumor T cells and suppression of the recruitment of $CD103^+$ DCs because of decreased expression of CCL4 (14). Consistent with the roles of the Wnt/β-catenin pathway in those previous reports, in this study, we found that the MMTV-Wnt1 mouse breast tumor model was resistant to anti-PD-1 antibody and that the number of $CD8^+$ cells was low in MMTV-Wnt1 tumor tissue (**Figs. 4C** and **5A** and **B**). However, E7386 showed synergistic antitumor activity in combination with anti-PD-1 antibody compared with each monotherapy treatment in the MMTV-Wnt1 mouse breast tumor model, where activated Wnt/β-catenin pathway might cause cold tumors. In fact, E7386 decreased the M2 macrophage population and increased lymphocyte infiltration into MMTV-Wnt1 tumor tissue. Although additional studies are needed to understand the precise immunomodulatory mechanism of E7386, we hypothesize that E7386 may alter the immunosuppressive tumor microenvironment to enhance the antitumor activity of anti-PD-1 antibody.

In conclusion, we demonstrated that E7386 exerted antitumor activity, an immunomodulatory effect, and synergistic antitumor activity in combination with anti-PD-1 antibody via inhibition of the interaction of β-catenin with CBP in human and in mouse preclinical tumor models with activation of the Wnt/β-catenin signaling pathway. On the basis of these preclinical results, E7386 monotherapy is currently being investigated in phase I clinical trials for patients with solid tumors in the United Kingdom and Japan (trial identifiers NCT03264664 and NCT03833700).

Authors' Disclosures

K. Yamada reports personal fees from Eisai Co., Ltd., during the conduct of the study and outside the submitted work. S. Inoue reports a patent for WO2015098853 issued and US20150175615 issued. Y. Yamamoto reports personal fees from Eisai Co., Ltd., during the conduct of the study and outside the submitted work, as well as has a patent for US2015175615 issued to Eisai Co., Ltd., and WO201598853 issued to Eisai Co., Ltd. K. Iso reports personal fees from Eisai Co., Ltd., during the conduct of the study and outside the submitted work, as well as has a patent for WO2015098853 issued and US20150175615 issued. H. Kamiyama reports personal fees from Eisai Co., Ltd., during the conduct of the study and outside the submitted work. A. Yamaguchi reports personal fees from Eisai Co., Ltd., during the conduct of the study and outside the submitted work. T. Kimura reports personal fees from Eisai Co., Ltd., during the conduct of the study and outside the submitted work. M. Uesugi reports personal fees from Eisai Co., Ltd., during the conduct of the study and outside the submitted work. M. Matsuki reports personal fees from Eisai Co., Ltd., during the conduct of the study and outside the submitted work, as well as has a patent for WO2018147275A1 pending. K. Nakamoto reports personal fees from Eisai. Co., Ltd., during the conduct of the study and outside the submitted work. H. Harada reports personal fees from Eisai Co., Ltd., during the conduct of the study and outside the submitted work. N. Yoneda reports personal fees from Eisai Co., Ltd., during the conduct of the study and outside the submitted work. A. Takemura reports personal fees from Eisai Co., Ltd., during the conduct of the study and outside the submitted work. I. Kushida reports personal fees from Eisai. Co., Ltd., during the conduct of the study and outside the submitted work. N. Wakayama reports personal fees from Eisai Co., Ltd., during the conduct of the study and outside the submitted work. Y. Kato reports personal fees from Eisai Co., Ltd., during the conduct of the study and outside the submitted work. T. Semba reports personal fees from Eisai Co., Ltd., during the conduct of the study and outside the submitted work. A. Yokoi reports personal fees from Eisai Co., Ltd., during the conduct of the study and outside the submitted work. M. Iwata reports personal fees from Eisai Co., Ltd., during the conduct of the study and outside the submitted work. T. Uenaka reports personal fees from Eisai Co., Ltd., during the conduct of the study and outside the submitted work. J. Matsui reports personal fees from Eisai Co., Ltd., during the conduct of the study and outside the submitted work. T. Matsushima reports personal fees from Eisai Co., Ltd., during the conduct of the study and outside the submitted work. T. Owa reports personal fees from Eisai Co., Ltd., during the conduct of the study and outside the submitted work. Y. Funahashi reports personal fees from Eisai Co., Ltd., during the conduct of the study and outside the submitted work. Y. Ozawa reports personal fees from Eisai Co., Ltd., during the conduct of the study and outside the submitted work, as well as has a patent for WO2016/204193 pending. No disclosures were reported by the other authors.

Authors' Contributions

K. Yamada: Validation, investigation, visualization, methodology, writing-original draft. **Y. Hori:** Validation, investigation, visualization, methodology. **S. Inoue:** Design and synthesis of E7386. **Y. Yamamoto:** Design and synthesis of E7386. **K. Iso:** Design and synthesis of E7386. **H. Kamiyama:** Validation, investigation, visualization, methodology. **A. Yamaguchi:** Validation, investigation, visualization, methodology. **T. Kimura:** Validation, investigation, visualization, methodology. **M. Uesugi:** Investigation, visualization, methodology. **J. Ito:** Formal analysis. **M. Matsuki:** Methodology. **K. Nakamoto:** Design and synthesis of E7386. **H. Harada:** Design and synthesis of E7386. **N. Yoneda:** Design and synthesis of E7386. **A. Takemura:** Design and synthesis of E7386. **I. Kushida:** Validation, investigation, methodology. **N. Wakayama:** Validation, investigation, methodology. **K. Kubara:** Methodology. **Y. Kato:** Validation, investigation, visualization, methodology, writing-review and editing. **T. Semba:** Conceptualization, project administration. **A. Yokoi:** Conceptualization, project administration. **M. Matsukura:** Conceptualization, project administration, design and synthesis of E7386. **T. Odagami:** Supervision. **M. Iwata:** Supervision. **A. Tsuruoka:** Supervision. **T. Uenaka:** Supervision. **J. Matsui:** Supervision. **T. Matsushima:** Supervision. **K. Nomoto:** Supervision. **H. Kouji:** Supervision. **T. Owa:** Supervision. **Y. Funahashi:** Supervision, writing-review and editing. **Y. Ozawa:** Conceptualization, validation, investigation, visualization, methodology, project administration, writing-review and editing.

Acknowledgments

We gratefully acknowledge Shuntaro Tsukamoto and Saori Ikeda (Eisai Co., Ltd.) and Sunplanet Co., Ltd., for their technical support with the experiments.

The costs of publication of this article were defrayed in part by the payment of page charges. This article must therefore be hereby marked *advertisement* in accordance with 18 U.S.C. Section 1734 solely to indicate this fact.

Received March 9, 2020; revised October 29, 2020; accepted December 28, 2020; published first January 6, 2021.

References

1. Clevers H, Nusse R. Wnt/β-catenin signaling and disease. Cell 2012;149:1192–205.
2. Nusse R, Clevers H. Wnt/β-catenin signaling, disease, and emerging therapeutic modalities. Cell 2017;169:985–99.
3. Zhan T, Rindtorff N, Boutros M. Wnt signaling in cancer. Oncogene 2017;36:1461–73.
4. Anastas JN, Moon RT. WNT signalling pathways as therapeutic targets in cancer. Nat Rev Cancer 2013;13:11–26.
5. Katoh M, Katoh M. Molecular genetics and targeted therapy of WNT-related human diseases (review). Int J Mol Med 2017;40:587–606.
6. Vilchez V, Turcios L, Marti F, Gedaly R. Targeting Wnt/β-catenin pathway in hepatocellular carcinoma treatment. World J Gastroenterol 2016;22:823–32.
7. Cancer Genome Atlas Network. Comprehensive molecular characterization of human colon and rectal cancer. Nature 2012;487:330–7.
8. Bible KC, Ryder M. Evolving molecularly targeted therapies for advanced-stage thyroid cancers. Nat Rev Clin Oncol 2016;13:403–16.
9. Lazar AJ, Tuvin D, Hajibashi S, Habeeb S, Bolshakov S, Mayordomo-Aranda E, et al. Specific mutations in the beta-catenin gene (CTNNB1) correlate with local recurrence in sporadic desmoid tumors. Am J Pathol 2008;173:1518–27.
10. Liu L, Zhi Q, Shen M, Gong FR, Zhou BP, Lian L, et al. FH535, a β-catenin pathway inhibitor, represses pancreatic cancer xenograft growth and angiogenesis. Oncotarget 2016;7:47145–62.
11. Sun X, Liu S, Wang D, Zhang Y, Li W, Guo Y, et al. Colorectal cancer cells suppress CD4+ T cells immunity through canonical Wnt signaling. Oncotarget 2017;8:15168–81.

12. Ganesh S, Shui X, Craig KP, Park J, Wang W, Brown BD, et al. RNAi-mediated β-catenin inhibition promotes T cell infiltration and antitumor activity in combination with immune checkpoint blockade. Mol Ther 2018;26:2567–79.
13. El-Sahli S, Xie Y, Wang L, Liu S. Wnt signaling in cancer metabolism and immunity. Cancers 2019;11:904.
14. Spranger S, Bao R, Gajewski TF. Melanoma-intrinsic β-catenin signalling prevents anti-tumour immunity. Nature 2015;523:231–5.
15. Ruiz de Galarreta M, Bresnahan E, Molina-Sánchez P, Lindblad KE, Maier B, Sia D, et al. β-catenin activation promotes immune escape and resistance to anti-PD-1 therapy in hepatocellular carcinoma. Cancer Discov 2019;8:1124–41.
16. Liu J, Pan S, Hsieh MH, Ng N, Sun F, Wang T, et al. Targeting Wnt-driven cancer through the inhibition of porcupine by LGK974. Proc Natl Acad Sci U S A 2013; 110:20224–9.
17. Gurney A, Axelrod F, Bond CJ, Cain J, Chartier C, Donigan L, et al. Wnt pathway inhibition via the targeting of Frizzled receptors results in decreased growth and tumorigenicity of human tumors. Proc Natl Acad Sci U S A 2012; 109:11717–22.
18. Jimeno A, Gordon M, Chugh R, Messersmith W, Mendelson D, Dupont J, et al. A first-in-human phase I study of the anticancer stem cell agent ipafricept (OMP-54F28), a decoy receptor for Wnt ligands, in patients with advanced solid tumors. Clin Cancer Res 2017;23:7490–7.
19. Krishnamurthy N, Kurzrock R. Targeting the Wnt/β-catenin pathway in cancer: update on effectors and inhibitors. Cancer Treat Rev 2018;62:50–60.
20. Harb J, Lin PJ, Hao J. Recent development of Wnt signaling pathway inhibitors for cancer therapeutics. Curr Oncol Rep 2019;21:12.
21. Kahn M. Can we safely target the WNT pathway? Nat Rev Drug Discov 2014;13: 513–32.
22. Moore KN, Gunderson CC, Sabbatini P, McMeekin DS, Mantia-Smaldone G, Burger RA, et al. A phase 1b dose escalation study of ipafricept (OMP54F28) in combination with paclitaxel and carboplatin in patients with recurrent platinum-sensitive ovarian cancer. Gynecol Oncol 2019;154:294–301.
23. Cui C, Zhou X, Zhang W, Qu Y, Ke X. Is β-catenin a druggable target for cancer therapy? Trends Biochem Sci 2018;43:623–34.
24. Emami KH, Nguyen C, Ma H, Kim DH, Jeong KW, Eguchi M, et al. A small molecule inhibitor of beta-catenin/CREB-binding protein transcription [corrected]. Proc Natl Acad Sci U S A 2004;101:12682–7.
25. Moser AR, Luongo C, Gould KA, McNeley MK, Shoemaker AR, Dove WF. ApcMin: a mouse model for intestinal and mammary tumorigenesis. Eur J Cancer 1995;31A:1061–4.
26. Tanaka T, Kohno H, Suzuki R, Hata K, Sugie S, Niho N, et al. Dextran sodium sulfate strongly promotes colorectal carcinogenesis in Apc(Min/+) mice: inflammatory stimuli by dextran sodium sulfate results in development of multiple colonic neoplasms. Int J Cancer 2006;118:25–34.
27. Bolger AM, Lohse M, Usadel B. Trimmomatic: a flexible trimmer for Illumina sequence data. Bioinformatics 2014;30:2114–20.
28. Dobin A, Davis CA, Schlesinger F, Drenkow J, Zaleski C, Jha S, et al. STAR: ultrafast universal RNA-seq aligner. Bioinformatics 2013;29:15–21.
29. Trapnell C, Roberts A, Goff L, Pertea G, Kim D, Kelley DR, et al. Differential gene and transcript expression analysis of RNA-seq experiments with TopHat and Cufflinks. Nat Protoc 2012;7:562–78.
30. Love MI, Huber W, Anders S. Moderated estimation of fold change and dispersion for RNA-seq data with DESeq2. Genome Biol 2014;15:550.
31. Nikolsky Y, Kirillov E, Zuev R, Rakhmatulin E, Nikolskaya T. Functional analysis of OMICs data and small molecule compounds in an integrated "knowledge-based" platform. Methods Mol Biol 2009;563:177–96.
32. Dezso Z, Nikolsky Y, Nikolskaya T, Miller J, Cherba D, Webb C, et al. Identifying disease-specific genes based on their topological significance in protein networks. BMC Syst Biol 2009;3:36.
33. Hsu CL, Huang YH, Hsu CT, Yang UC. Prioritizing disease candidate genes by a gene interconnectedness-based approach. BMC Genomics 2011;12:S25.
34. Vanunu O, Magger O, Ruppin E, Shlomi T, Sharan R. Associating genes and protein complexes with disease via network propagation. PLoS Comput Biol 2010;6:e1000641.
35. Fakhry CT, Choudhary P, Gutteridge A, Sidders B, Chen P, Ziemek D, et al. Interpreting transcriptional changes using causal graphs: new methods and their practical utility on public networks. BMC Bioinformatics 2016;17:318.
36. Newman AM, Liu CL, Green MR, Gentles AJ, Feng W, Xu Y, et al. Robust enumeration of cell subsets from tissue expression profiles. Nat Methods 2015; 12:453–7.
37. Wolf D, Rodova M, Miska EA, Calvet JP, Kouzarides T. Acetylation of beta-catenin by CREB-binding protein (CBP). J Biol Chem 2002;277:25562–7.
38. Rishikaysh P, Dev K, Diaz D, Qureshi WM, Filip S, Mokry J. Signaling involved in hair follicle morphogenesis and development. Int J Mol Sci 2014;15:1647–70.
39. Hendaoui I, Tucker RP, Zingg D, Bichet S, Schittny J, Chiquet-Ehrismann R. Tenascin-C is required for normal Wnt/β-catenin signaling in the whisker follicle stem cell niche. Matrix Biol 2014;40:46–53.
40. Nuñez F, Bravo S, Cruzat F, Montecino M, De Ferrari GV. Wnt/β-catenin signaling enhances cyclooxygenase-2 (COX2) transcriptional activity in gastric cancer cells. PLoS One 2011;6:e18562.
41. Tetsu O, McCormick F. Beta-catenin regulates expression of cyclin D1 in colon carcinoma cells. Nature 1999;398:422–6.
42. Xu L, Corcoran RB, Welsh JW, Pennica D, Levine AJ. WISP-1 is a Wnt-1- and beta-catenin-responsive oncogene. Genes Dev 2000;14:585–95.
43. Tsukamoto AS, Grosschedl R, Guzman RC, Parslow T, Varmus HE. Expression of the int-1 gene in transgenic mice is associated with mammary gland hyperplasia and adenocarcinomas in male and female mice. Cell 1988;55: 619–25.
44. Zemans RL, McClendon J, Aschner Y, Briones N, Young SK, Lau LF, et al. Role of β-catenin-regulated CCN matricellular proteins in epithelial repair after inflammatory lung injury. Am J Physiol Lung Cell Mol Physiol 2013; 304:L415–27.
45. Li M, Knight DA, A Snyder L, Smyth MJ, Stewart TJ. A role for CCL2 in both tumor progression and immunosurveillance. Oncoimmunology 2013;2: e25474.
46. Li Y, Patel SP, Roszik J, Qin Y. Hypoxia-driven immunosuppressive metabolites in the tumor microenvironment: new approaches for combinational immunotherapy. Front Immunol 2018;9:1591.
47. Yang Y, Ye YC, Chen Y, Zhao JL, Gao CC, Han H, et al. Crosstalk between hepatic tumor cells and macrophages via Wnt/β-catenin signaling promotes M2-like macrophage polarization and reinforces tumor malignant behaviors. Cell Death Dis 2018;9:793.
48. Xu R, Li Y, Yan H, Zhang E, Huang X, Chen Q, et al. CCL2 promotes macrophages-associated chemoresistance via MCPIP1 dual catalytic activities in multiple myeloma. Cell Death Dis 2019;10:781.
49. Sharma P, Allison JP. The future of immune checkpoint therapy. Science 2015; 348:56–61.
50. Bonaventura P, Shekarian T, Alcazer V, Valladeau-Guilemond J, Valsesia-Wittmann S, Amigorena S, et al. Cold tumors: a therapeutic challenge for immunotherapy. Front Immunol 2019;10:168.